NATIONAL ADVISORY COMMITTEE FOR AERONAUTICS

TECHNICAL NOTE 2323

THEORETICAL INVESTIGATION OF SUBMERGED INLETS AT LOW SPEEDS

By Alvin H. Sacks and John R. Spreiter

Ames Aeronautical Laboratory
Moffett Field, Calif.

NACA

Washington

August 1951

NATIONAL ADVISORY COMMITTEE FOR AERONAUTICS

TECHNICAL NOTE 2323

THEORETICAL INVESTIGATION OF SUBMERGED INLETS AT LOW SPEEDS

By Alvin H. Sacks and John R. Spreiter

SUMMARY

The general characteristics of the flow field in a submerged air inlet are investigated by theoretical, wind-tunnel, and visual-flow studies.

Equations are developed for calculating the laminar and turbulent boundary-layer growth along the ramp floor for parallel, divergent, and convergent ramp walls, and a general equation is derived relating the boundary-layer pressure losses to the boundary-layer thickness. It is demonstrated that the growth of the boundary layer on the floor of the divergent-ramp inlet is retarded and that a vortex pair is generated in such an inlet. Functional relationships are established between the pressure losses in the vortices and the geometry of the inlet.

A general discussion of the boundary layer and vortex formations is included, in which variations of the various losses and of the incremental external drag with mass-flow ratio are considered. Effects of compressibility are also discussed.

INTRODUCTION

Among the various types of air inlets considered for use with aircraft internal flow systems is the submerged or flush inlet. As a result of extensive experimental research by the NACA at its Ames Aeronautical Laboratory, reported in several papers and reviewed in reference 1, a particular inlet of this type was developed (fig. 1) exhibiting pressure recovery and drag characteristics which make it suitable for application to aircraft.

In contrast to the nose inlet and the wing leading-edge inlet, the submerged inlet does not operate in essentially free-stream air. The

air entrained by the submerged inlet suffers pressure losses, the magnitude and distribution of which may be drastically affected by the geometry of the approach ramp.[1] The design of this approach ramp, in both profile and plan form, is a problem basic to the further development of submerged inlets in general. Although some of the basic concepts to be presented here regarding the flow in submerged inlets are known (see reference 1), the purpose of the present paper is to analyze theoretically the relative importance of the various design parameters and to indicate, insofar as possible, methods for calculating their effects on the over-all performance of a submerged inlet.

LIST OF IMPORTANT SYMBOLS

A_D	duct entrance area
b	local width of ramp
C	fraction of vortex losses entering duct
d	depth of duct entrance measured between lip and ramp floor
h	local depth of ramp
H	boundary-layer-shape parameter $\left(\frac{\delta^*}{\theta}\right)$
H_o	free-stream total pressure
H_1	local total pressure
l	ramp length
m_1/m_o	mass-flow ratio $\left(\frac{\rho_1 V_1}{\rho_o u_o}\right)$
M	Mach number
p	local static pressure
p_o	free-stream static pressure
q	peripheral velocity in vortex field
q_o	free-stream dynamic pressure $\left(\frac{1}{2}\rho u_o^2\right)$
R	Reynolds number

[1] The ramp is here defined as the inclined passageway leading to the duct entrance. (See fig. 1.) It is composed of a floor and two side walls.

r	radial coordinate
r_c	radius of vortex core
s	width of fuselage surface from which boundary layer enters one vortex core
u	velocity component inside the floor boundary layer in local stream direction
u_o	free-stream velocity
u_1	local velocity at edge of the boundary layer
$\overline{V}$	velocity vector
V_1	average velocity at duct entrance
v	velocity component inside the floor boundary layer perpendicular to the ramp floor
w	velocity component perpendicular to ramp wall
w_1	velocity component inside the boundary layer perpendicular to u and v
x,y	rectangular coordinates
α	local ramp angle relative to the free-stream direction
Γ	circulation
γ	$\int_o^1 \left(1 - \frac{u}{u_1}\right) d\eta$
ΔC_D	incremental drag coefficient due to air inlet
ΔH	loss in total pressure, $\left(H_o - H_1\right)$
$\frac{\overline{\Delta H}}{q_o}$	nondimensional average loss in total pressure defined in equation (1)
δ	boundary-layer thickness
δ^*	boundary-layer displacement thickness
η	$\frac{y}{\delta}$

θ boundary-layer momentum thickness

Λ nondimensional parameter involving Reynolds number and pressure gradient

$$\left[\left(\frac{u_1\theta}{\nu}\right)^{1/4}\left(\frac{du_1}{dr}\frac{\theta}{u_1}\right)\right]$$

λ $\frac{\delta^2}{\nu}\frac{du_1}{dx}$

μ friction coefficient

ν kinematic viscosity $\left(\frac{\mu}{\rho}\right)$

ρ mass density

ρ_o free-stream mass density

ρ_1 average mass density at duct entrance

τ shear stress

φ polar coordinate

Ω $\int_o^1 \left(\frac{u}{u_1} - \frac{u^2}{u_1^2}\right) d\eta$

ω local angle of ramp-wall divergence

ζ nondimensional shear-stress variable

Subscripts

BL boundary layer

BLC boundary-layer control on fuselage due to inlet

BLF ramp floor boundary layer

BLS fuselage surface boundary layer entrained in vortex cores

e contributing to external drag

i contributing to internal pressure losses

SEP due to separation of fuselage boundary layer at the edges of the inlet

V vortex

THE FLOW IN SUBMERGED INLETS

General Observations

The complex three-dimensional character of the flow in a submerged inlet, involving appreciable viscous effects, makes direct mathematical analysis difficult. In order to indicate the nature of the idealizations to be made and to justify the simplifications introduced in the solution of the problem, the present section is concerned with a qualitative examination of the potential and viscous flow fields and their interaction.

In general, there are three classes of plan forms possible for an approach ramp (see sketch) – it may have parallel walls (a), divergent walls (b), or convergent walls (c).

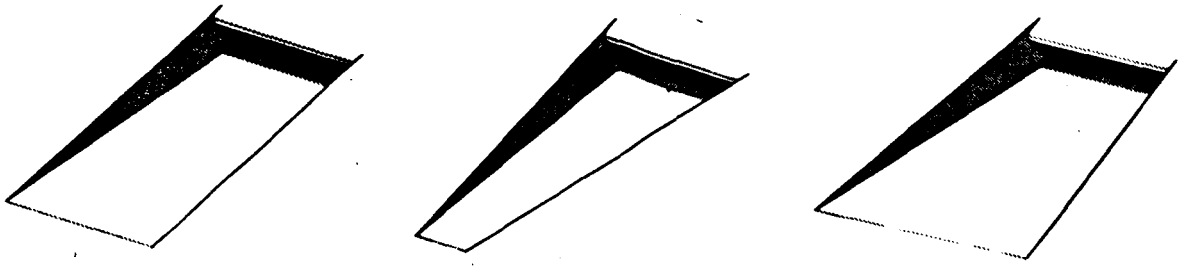

(a) parallel walls (b) divergent walls (c) convergent walls

It appears that the flow in the parallel-walled ramp can generally be approximated with a two-dimensional analysis, at least for the case of moderate mass-flow ratios. The flow in the divergent-walled ramp, however, exhibits two important differences from that of the parallel-walled ramp. These differences rule out the use of a two-dimensional analysis even as a first approximation. First, the boundary layer cannot be expected to behave as one in a two-dimensional flow since the flow near the floor of this ramp is divergent at all mass-flow ratios. Second, the external stream, being no longer parallel to the ramp walls, must flow over the top of the walls into the inlet. It is well known that, if the velocity over such a corner is to remain finite, the formation of a vortex sheet is necessary.[2] Thus, a vortex sheet is formed along each edge of the divergent-walled inlet. The study of the flow field in such an inlet, then, involves not only the behavior of the boundary layer but also the behavior of the vortex sheets.

Since a knowledge of the potential flow is required to determine the character of the boundary layer, it is first necessary to consider

[2] This was in fact stated by Prandtl (reference 2) as a fundamental theorem: "Projecting edges of bodies are, for a flow meeting them transversely, always lines of confluence (and therefore as a rule origins of vortex sheets)."

the general behavior of the vortex sheets and their influence on the flow. Well forward in the divergent ramp, the vortex sheets, having just left the ramp walls, are still essentially flat, as shown in the sketch:

This arrangement of free vortices, however, cannot persist farther downstream in the inlet since each vortex filament making up the sheet, being free to move, must move in accordance with the velocities induced upon it by all the other vortices present in the fluid. The induced velocities are such that the filaments will move into the ramp and roll up as they proceed toward the duct entrance in a manner much as shown in the sketch.

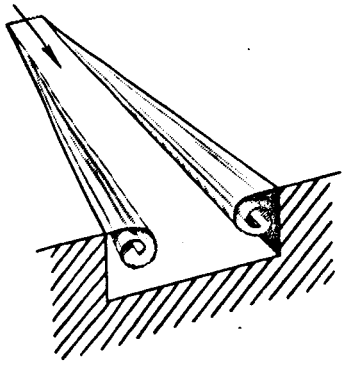

If the process described above were permitted to continue far downstream without further change in inlet cross section (i.e., in a parallel-walled open channel extending downstream from the divergent ramp), the two sheets would eventually become completely rolled up into two more or less cylindrical vortex regions.

The third possible ramp plan form, the convergent ramp, presents a problem of analysis similar to that of the divergent ramp in several respects. First, the boundary-layer growth along the ramp floor is affected by the convergence of the flow. Second, due to the non-parallel ramp walls, there is again the possibility of the formation and rolling up of a pair of vortex sheets. In this case, however, if such a vortex pair is formed, the rolling up will generally occur outside the inlet (due to the upward flow over the ramp edges) and therefore have little influence on the internal pressure recovery of the inlet.

Since the divergent-ramp inlet represents the most general case in that its pressure recovery is affected by all of the influences discussed, and since it has shown promise experimentally from the standpoint of

over-all performance, the bulk of the present analysis will be developed for this case. However, as will be mentioned from time to time, the equations to be derived will be generally applicable to all three classes of ramp plan forms unless a statement to the contrary is made.

Visual-Flow Studies

The general observations made in the preceding paragraphs regarding the vortex formations have been substantiated by visual-flow studies of a divergent-ramp inlet. These tests were made in a water tank (fig. 2) by driving the model vertically down into the water, the surface of which was dusted with fine aluminum powder. The motion in transverse planes was observed by photographing the water surface with a motion-picture camera. A typical series of photographs is shown in figure 3, in which the formation and rolling up of the vortex sheets are clearly demonstrated.

Behavior of the Boundary Layer

The boundary layers of interest in the submerged inlet are those developed on the ramp floor and the ramp walls. However, since the boundary layer on the ramp wall has a zero initial thickness and develops over a relatively small wetted area, its contribution to the losses in the inlet is not likely to be significant unless the ramp divergence is so large that the flow separates from the walls.[3] Since the floor boundary layer covers a larger wetted area and may have a substantial initial thickness, it is of primary concern. Therefore, equations will be developed for the calculation of the boundary-layer growth along this surface.

As might be anticipated, the rate of growth of the floor boundary layer will be shown to depend upon the pressure distribution and upon the divergence (or convergence) of the flow. The pressure distribution, in turn, is determined by the inlet geometry and by the mass-flow ratio; whereas the divergence of the flow is primarily influenced by the plan form of the inlet and by the induced velocities due to the rolled-up vortices.

---

[3] Calculations have indicated that the order of magnitude of the wall boundary-layer loss is 5 to 10 percent of that due to the floor boundary layer.

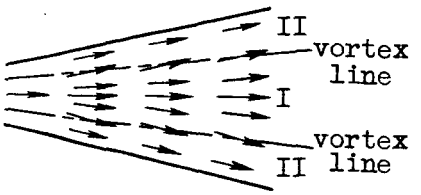

At the surface of the divergent-ramp floor, all the velocities induced by the vortices are in directions away from the center line of the ramp. This effect reaches a maximum underneath the centers of the rolled-up vortex sheets. Thus, the flow along the floor of the divergent ramp may be divided into two general types of regions, as shown in the sketch. The effect of the vortices on the flow in region I is essentially to increase the divergence of the flow; whereas that in regions II is to reduce the divergence of the flow. It will be demonstrated in the analysis that the boundary-layer growth is accelerated by convergence of the flow and retarded by divergence of the flow. It can be seen, therefore, that the floor boundary layer will grow most rapidly near the ramp walls, while toward the center of the ramp it will grow more slowly or may, in fact, diminish in thickness as the duct entrance is approached. In any case, the boundary layer on the floor of a divergent ramp will be thinnest near the center line and thickest toward the ramp walls.

Inlet Pressure Losses

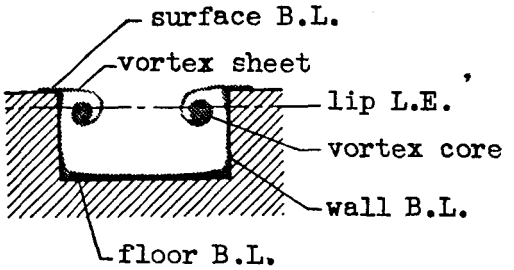

From the foregoing discussion, a qualitative picture can be constructed of the flow which is finally developed in the inlet just ahead of the duct entrance at moderately high mass-flow ratios.[4] Such a picture is presented in cross section in the sketch. The main sources of pressure losses in the duct entrance, then, are the floor boundary layer and some portion of the vortex cores (including entrained surface boundary layer), depending upon the relative locations of the duct lip and the vortices.

It has become customary in low-speed inlet work to express pressure loss as the ratio of the total-pressure loss to the free-stream impact pressure. Since it is a practical certainty that the flow in a duct is not uniform and that the losses vary from point to point across the inlet, it is desirable to compute an "effective" pressure loss which is indicative of the over-all performance of the inlet. That is, it is

[4] Effects of changes in mass-flow ratio will be discussed in a later section.

desired to determine the difference between the total pressure in the free stream and that which would be measured in a plenum chamber after perfect diffusion. While the exact determination of such an effective total-pressure loss is, in general, a difficult problem, several methods have been proposed which involve averaging the local total-pressure losses in a variety of ways. Among those that have been used are a simple area average and averages "weighted" according to the local mass flows or the logarithm of the local mass flows. A theoretical analysis of the diffusion in a straight pipe of flows having initially nonuniform velocity distributions indicates that a simple area average, in addition to being the simplest to calculate, yields results which are generally as accurate as (and in some cases more accurate than) those obtained with the more complicated weighted averages.

In accordance with the results of the theoretical pipe-flow analysis, the pressure-loss parameter in this report will be determined on the basis of a simple area average. Thus at low speeds,

$$\left(\frac{H_o - H_1}{H_o - p_o}\right)_{av} \approx \left(\frac{H_o - H_1}{q_o}\right)_{av} = \left(\frac{\overline{\Delta H}}{q_o}\right) = \frac{1}{A_D}\int\left(\frac{\Delta H}{q_o}\right) dA \qquad (1)$$

where A_D is the duct-entrance area. The portion of the quantity $(\overline{\Delta H}/q_o)$ which is taken into the duct entrance (internal loss) can be expressed as the sum of the losses discussed. That is,

$$\left(\frac{\overline{\Delta H}}{q_o}\right)_i = \left(\frac{\overline{\Delta H}}{q_o}\right)_{BLF} + C\left[\left(\frac{\overline{\Delta H}}{q_o}\right)_V + \left(\frac{\overline{\Delta H}}{q_o}\right)_{BLS}\right] \qquad (2)$$

where C is the fraction of the bracketed losses taken internally. The ensuing sections of this paper will be primarily concerned with the theoretical determination of the losses indicated in equation (2). The external loss $(\overline{\Delta H}/q_o)_e$ will also be investigated.

VORTEX INVESTIGATION

A detailed mathematical analysis of the rolling-up process by which the vortex sheets approach their stable form would involve a study of the time history of each vortex filament leaving the ramp walls. Such a detailed study may not be necessary, however, since the major interest for the present problem is the determination of quantities which will influence the magnitude and distribution of the pressure losses in the inlet. It will be shown in the analysis that the magnitude of the pressure losses in the vortex regions themselves is determined (within the limitations of the theory) solely by the value of the circulation. The

purpose here is therefore to develop an expression for the vortex circulation at any station in the inlet. Toward this end, recourse will be had to the method of dimensional analysis, which will furnish much of the desired information without undue complication.

Determination of Circulation

Consider a divergent-ramp inlet of arbitrary geometry mounted in an infinite flat wall as shown in the sketch.

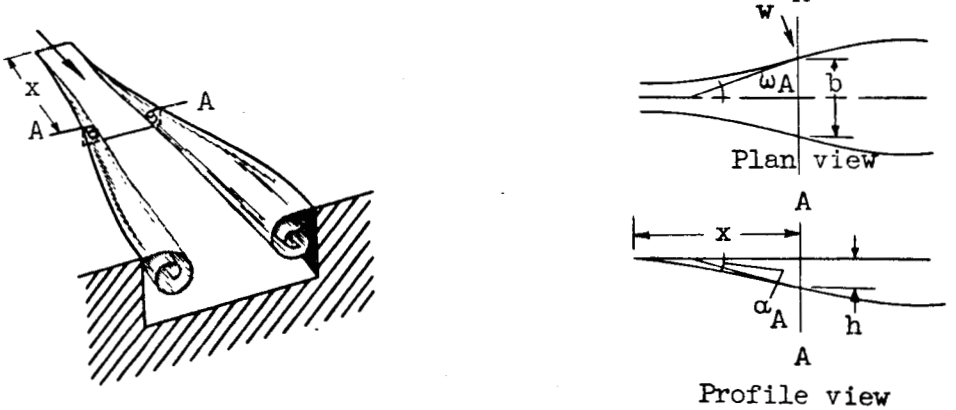

Suppose now that the circulation $d\Gamma$ shed from one wall in an element of length dx in the stream direction is taken to be a function of the local changes in width and depth of the inlet, the free-stream Reynolds number and Mach number, and the mass-flow ratio of the duct. This statement may be expressed in functional notation as

$$d\Gamma = d\Gamma\,(db,\ dh,\ R,\ M,\ m_1/m_o) \tag{3}$$

The analysis will be concerned with an inlet operating at a constant Reynolds number and Mach number, and the effect of mass-flow ratio will be taken into account by the introduction of another variable, namely, the velocity component w perpendicular to the ramp wall at the edge of the ramp. (See preceding sketch.) Equation (3) is thus reduced to

$$d\Gamma = d\Gamma\,(w,\ db,\ dh) \tag{4}$$

Dimensional analysis shows that there are only two basic dimensionless combinations of these four variables. They are

$$\frac{d\Gamma}{w\,dh} \quad \text{and} \quad \frac{db}{dh}$$

Therefore, there is some function Φ of these variables which satisfies the equation

$$\Phi\left(\frac{d\Gamma}{w\,dh}, \frac{db}{dh}\right) = 0 \tag{5}$$

That is,

$$\frac{d\Gamma}{w\,dh} = \Psi\left(\frac{db}{dh}\right)$$

or

$$d\Gamma = w\,dh\,\Psi\left(\frac{db}{dh}\right) \tag{6}$$

Now, from the geometry of the inlet (see preceding sketch), expressions can be written for dh and db in terms of the local angles α and ω and the differential distance dx, thus

$$dh = dx \tan \alpha$$

$$db = 2dx \tan \omega$$

or, for small angles,

$$dh = \alpha\,dx$$

$$db = 2\omega\,dx$$

The velocity component w is a function of the free-stream velocity, the mass-flow ratio, and the geometry of the inlet. Similarity considerations indicate that it is reasonable to assume that w is linearly dependent upon the free-stream velocity and is composed of two additive parts, one proportional to ω and the other to α, that is,

$$w = (K_1\,\omega + K_2\,\alpha)u_o \tag{7}$$

where K_1 and K_2 depend only upon the mass-flow ratio. Since the ramp angle α is always positive, it is apparent that under this assumption if ω equals 0 (parallel walls) there will still be some vorticity shed into the inlet; whereas at sufficiently large negative values of ω (convergent walls), the velocity w vanishes and then takes on negative values which have no meaning in this analysis.

By use of the substitutions just discussed, equation (6) can be rewritten

$$d\Gamma = u_o \alpha \, dx \cdot (K_1 \omega + K_2 \alpha) \psi\left(\frac{2\omega}{\alpha}\right)$$

or

$$\frac{d\Gamma}{dx} = u_o \alpha^2 \cdot \left(K_1 \frac{\omega}{\alpha} + K_2\right) f\left(\frac{\omega}{\alpha}\right) \tag{8}$$

The circulation at any station (say $x=l$) is then given by

$$\Gamma(l) = u_o \int_o^l \alpha^2 \cdot \left(K_1 \frac{\omega}{\alpha} + K_2\right) f\left(\frac{\omega}{\alpha}\right) dx \tag{9}$$

Before the integration can be carried out by graphical or numerical methods, there remains the problem of determining K_1, K_2, and f.

Since the effect of variations in mass-flow ratio is primarily one of blockage at the duct entrance, it is apparent that such an effect will be confined largely to stations near the duct lip; that is, the variation of K_1 and K_2 with m_1/m_o will be small over most of the ramp length. Hence, for smoothly faired inlets the net effect of mass-flow ratio on the integrated circulation Γ will be small. Thus, except for small changes due to mass-flow ratio, equation (9) can be written

$$\Gamma(l) = u_o \int_o^l \alpha^2 g\left(\frac{\omega}{\alpha}\right) dx \tag{10}$$

where g is now an unspecified function of a single variable ω/α. Within the assumptions of this analysis, the function g can be determined from a single test series involving divergent-ramp inlets of linear geometry since for this case equation (10) can be written

$$g\left(\frac{\omega}{\alpha}\right) = \frac{\Gamma(l)}{u_o \alpha^2 l}$$

In equation (10), the circulation varies directly with the free-stream velocity u_o. However, this is due to the assumption that the inlet was mounted in an infinite flat wall. If, on the other hand, the

inlet were mounted in a fuselage, the velocity to be used would be a mean local velocity u_1 over the region in which the inlet is installed. Thus, equation (10) would be

$$\Gamma = u_1 \int_0^l \alpha^2 g\left(\frac{w}{\alpha}\right) dx \tag{11}$$

Due to the nature of the assumptions made in this section with regard to the velocity w, the equations developed for the vortex circulation are not generally applicable to convergent-ramp inlets.

Vortex Pressure Losses

A simplified analysis will be carried out here to investigate the pressure characteristics of the vortices and their effect on the losses in total pressure. In particular, it is desired to determine an expression for the vortex pressure loss $(\overline{\Delta H}/q_0)_V$. It will be assumed at the outset that the inlet is sufficiently slender that velocity gradients in the stream direction are negligibly small in comparison with those in the transverse directions. In addition, each of the actual vortex regions will be replaced by an idealized potential vortex containing a rotational core of finite diameter. This implies that the total-pressure losses in each vortex will be unaffected by the presence of the other vortex or by the bounding surfaces. The analysis is therefore equivalent to determining the pressure losses in a single cylindrical vortex rotating in a uniform incompressible stream flowing parallel to the axis of rotation, as illustrated in the following sketches:

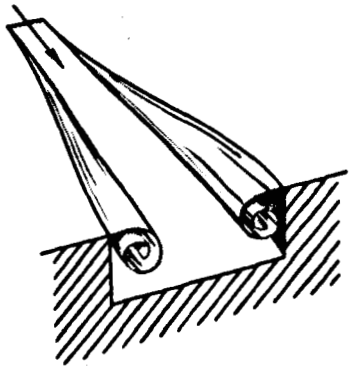

Actual inlet vortex flow in cross section

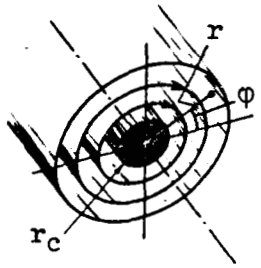

Approximation to each vortex

With the preceding assumptions, the general expression for the losses in both vortices can be written

$$\left(\frac{\overline{\Delta H}}{q_o}\right)_V = \frac{2}{A_D} \int \left(\frac{\Delta H}{q_o}\right) dA \tag{12}$$

Moreover, since vortex total-pressure losses appear only inside the vortex cores,[5] equation (12) can be expanded to give

$$\left(\frac{\overline{\Delta H}}{q_o}\right)_V = \frac{2}{A_D q_o} \int_o^{2\pi} \int_o^{r_c} (H_o - H_1)\, r\, dr\, d\varphi \tag{13}$$

where r_c is the radius of the vortex core.

The total pressure H_1 anywhere in the fluid is expressed in general as the sum of the local static and dynamic pressures.

$$H_1 = p + \frac{1}{2} \rho\, (u_o^2 + q^2) \tag{14}$$

where u_o is the velocity of the uniform stream (parallel to the vortex axis) and q is a peripheral velocity in the vortex. The condition to be satisfied by the transverse velocities q is that the pressures must everywhere be balanced by the centrifugal force; that is,

$$\frac{dp}{dr} = \rho \frac{q^2}{r} \tag{15}$$

Therefore, the radial variation of total pressure through the vortex can be found by differentiating equation (14), using the relationship of equation (15), thus

$$\frac{dH_1}{dr} = \frac{dp}{dr} + \frac{d}{dr} \left(\frac{1}{2} \rho\, q^2\right)$$

$$= \rho \left(\frac{q^2}{r} + q \frac{dq}{dr}\right) \tag{16}$$

[5] The vortex core will be defined in this analysis as a circular region surrounding the vortex center in which the peripheral velocities deviate from those of the potential vortex.

This equation can be integrated to give an expression for the total pressure at any point in the vortex. In general,

$$H_1(r) - H_1(\infty) = H_1(r) - H_o = \rho \int_{\infty}^{r} \left(\frac{q^2}{r} + q \frac{dq}{dr} \right) dr$$

$$= \rho \int_{\infty}^{r_c} \left(\frac{q^2}{r} + q \frac{dq}{dr} \right) dr + \rho \int_{r_c}^{r} \left(\frac{q^2}{r} + q \frac{dq}{dr} \right) dr \tag{17}$$

The first integral vanishes since $q = \Gamma/2\pi r$ everywhere outside the core, giving

$$H_1(r) - H_o = \rho \int_{r_c}^{r} \left(\frac{q^2}{r} + q \frac{dq}{dr} \right) dr \tag{18}$$

Substitution of the above expression (with limits reversed) into equation (13) yields

$$\left(\frac{\overline{\Delta H}}{q_o} \right)_V = \frac{4\pi\rho}{A_D q_o} \int_o^{r_c} r \, dr \int_r^{r_c} \left[\frac{q^2(r_o)}{r_o} + q(r_o) \frac{dq(r_o)}{dr_o} \right] dr_o \tag{19}$$

Now, by reversing the order of integration, equation (19) can be written

$$\left(\frac{\overline{\Delta H}}{q_o} \right)_V = \frac{4\pi\rho}{A_D q_o} \int_o^{r_c} \left(\frac{q^2}{r_o} + q \frac{dq}{dr_o} \right) dr_o \int_o^{r_o} r \, dr \tag{20}$$

which reduces to

$$\left(\frac{\overline{\Delta H}}{q_o} \right)_V = \frac{8\pi}{A_D u_o^2} \int_o^{r_c} \frac{1}{2} \left(q^2 r_o + q \, r_o^2 \frac{dq}{dr_o} \right) dr_o \tag{21}$$

Observing that the expression in the parentheses is now a perfect differential, equation (21) can be integrated directly to give

$$\left(\frac{\overline{\Delta H}}{q_o}\right)_V = \frac{4\pi}{A_D u_o^2}\left[\frac{1}{2}\,q^2(r_o) \times r_o^2\right]_o^{r_c} = \frac{2\pi}{A_D u_o^2}\left[q^2(r_c) \times r_c^2\right] \qquad (22)$$

But at the edge of the core the peripheral velocity q is

$$q(r_c) = \frac{\Gamma}{2\pi r_c}$$

Thus, the total-pressure loss in the vortex pair is finally given by

$$\left(\frac{\overline{\Delta H}}{q_o}\right)_V = \frac{1}{2\pi A_D}\left(\frac{\Gamma}{u_o}\right)^2 \qquad (23)$$

It is evident from equation (23) that, within the limitations of the assumptions made, the integrated vortex pressure losses are independent of the size and velocity distribution of the vortex cores, and depend only upon the circulation.

BOUNDARY-LAYER INVESTIGATION

Boundary-Layer Analysis[6]

As was mentioned earlier, the boundary layer of primary interest in calculating inlet pressure losses is that on the floor of the ramp. In order to calculate the boundary-layer growth in a ramp having non-parallel walls, it is convenient to construct a variation of the Kármán momentum equation which will apply to a diverging flow over a flat plate. For this analysis, the following assumptions are made in addition to those usually used in boundary-layer theory:

1. Incompressible fluid

[6]This section presents (with some modification) a condensation of a thesis submitted by the senior author to Cornell University in 1949 for the degree, Master of Aeronautical Engineering.

2. Straight divergence of the ramp
3. The flow near the ramp floor is in radial lines emanating from the vertex of the straight divergent ramp

There are three possibilities regarding the character of the boundary layer along the ramp floor: (1) The boundary layer is laminar over the entire ramp; (2) the boundary layer is turbulent over the entire ramp; or (3) transition occurs somewhere on the ramp. The first two cases will be treated individually and the third will be constructed by combining the first two.

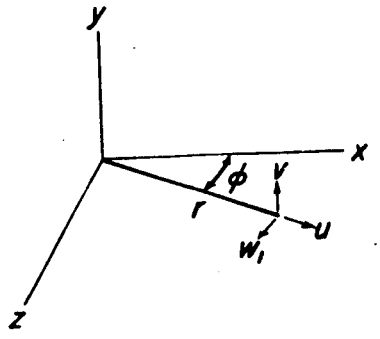

With the assumption of radial flow, it is convenient to introduce a cylindrical coordinate system to use throughout the analysis. Since the tangential velocity w_1 (see sketch) is identically zero everywhere in a radial flow, the equation of continuity can be expressed in cylindrical coordinates by

$$\operatorname{div} \overline{V} = \frac{1}{r} \frac{\partial}{\partial r} (ru) + \frac{\partial v}{\partial y} = 0 \tag{24}$$

while the boundary-layer equation in this coordinate system is given by

$$u \frac{\partial u}{\partial r} + v \frac{\partial u}{\partial y} = - \frac{1}{\rho} \frac{dp}{dr} + \frac{1}{\rho} \frac{d\tau}{dy} \tag{25}$$

(See reference 3.) These equations will be used to derive a momentum equation for radial flow which can be integrated to give an expression for the boundary-layer growth along the ramp floor.

Equation (24) can be rewritten as

$$v = - \int_0^{\delta} \frac{1}{r} \frac{\partial}{\partial r} (ru) \, dy \tag{26}$$

If this substitution is made in equation (25), noting that

$$v \frac{\partial u}{\partial y} = \frac{\partial}{\partial y} (uv) - u \frac{\partial v}{\partial y}$$

and that

$$\int_0^\delta \frac{\partial}{\partial y}(uv)\,dy = uv\Big]_0^\delta = u_1 \int_0^\delta \left(-\frac{\partial u}{\partial r} - \frac{u}{r}\right) dy$$

then equation (25) can be integrated over the boundary-layer thickness and reduced to the form

$$\frac{\partial}{\partial r}\left(r\int_0^\delta \rho u^2 dy\right) - u_1 \frac{\partial}{\partial r}\left(r\int_0^\delta \rho\, u\, dy\right) = -r\delta\frac{dp}{dr} - r\tau_0 \qquad (27)$$

where u_1 is the velocity at the edge of the boundary layer and τ_0 is the value of τ at $y = 0$. Further, by introducing the definitions of momentum thickness and displacement thickness of the boundary layer

$$\theta = \frac{1}{\rho u_1^2}\int_0^\delta \rho u(u_1 - u)\,dy$$

and

$$\delta^* = \frac{1}{\rho u_1}\int_0^\delta \rho(u_1 - u)\,dy$$

and noting that at the edge of the boundary layer equation (25) gives

$$\frac{dp}{dr} = -\rho u_1 \frac{du_1}{dr}$$

equation (27) can be written in terms of momentum and displacement thicknesses as

$$\rho u_1^2 \frac{d\theta}{dr} + \rho u_1 \frac{du_1}{dr}(2\theta + \delta^*) + \rho u_1^2 \frac{\theta}{r} = \tau_0 \qquad (28)$$

This is a momentum equation which reduces to that given by Karman (reference 4) for the case when r is infinite (parallel flow).

Laminar Case

For the laminar case, equation (28) can be put into a form involving only the total boundary-layer thickness δ by using the standard functional notation for the velocity profile inside the boundary layer

$$u = u_1 f\left(\frac{y}{\delta}, r\right) = u_1 f(\eta, r)$$

That is, the momentum and displacement thicknesses are replaced by the expressions

$$\theta = \delta\Omega \quad ; \quad \delta^* = \delta\gamma \tag{29}$$

where

$$\Omega \equiv \int_0^1 (f - f^2)\, d\eta \quad ; \quad \gamma \equiv \int_0^1 (1 - f)\, d\eta$$

Note that Ω and γ are simply functions of r which are defined once the variation of f with η (i.e., the velocity profile) is known. If it is further noted that

$$\tau_0 = \mu\left(\frac{\partial u}{\partial y}\right)_0 = \mu \frac{\partial}{\partial y}\left[u_1 f(\eta, r)\right] = \frac{\mu u_1 \frac{d}{d\eta}[f(0, r)]}{\delta} = \frac{\mu u_1 \beta}{\delta}$$

where

$$\beta \equiv \frac{d}{d\eta}[f(0, r)]$$

then equation (28) becomes

$$\delta^2 \left[u_1^2 \frac{d\Omega}{dr} + u_1 \frac{du_1}{dr}(2\Omega + \gamma) + \frac{u_1^2 \Omega}{r} \right] = \nu u_1 \beta - \frac{u_1^2 \Omega}{2} \frac{\partial}{\partial r}(\delta^2) \tag{30}$$

where $\nu = \mu/\rho$.

If a Pohlhausen velocity profile is assumed to exist in the laminar boundary layer, that is,

$$\frac{u}{u_1} = f = g\eta + c\eta^2 + d\eta^3 + e\eta^4$$

where $g = \frac{12 + \lambda}{6}$; $c = -\frac{\lambda}{2}$; $d = -\frac{4 - \lambda}{2}$; $e = \frac{6 - \lambda}{6}$; and $\lambda = \frac{\delta^2}{\nu}\frac{du_1}{dr}$;

the expressions for Ω, β, and γ are immediately found to be

$$\Omega = A+B\lambda+C\lambda^2$$

$$\beta = D+E\lambda$$

$$\gamma = F+G\lambda$$

where A, B, C, D, E, F, and G are constants. This leads to the final expression for the laminar boundary-layer growth (in dimensionless form)

$$\frac{d\epsilon}{d\xi} = \frac{2\delta}{l}\frac{d\delta}{dr} = \frac{\frac{2\beta}{\Omega UR} - \frac{2\epsilon}{\Omega}\left[\frac{\Omega}{\xi} + \frac{1}{U}\frac{dU}{d\xi}(2\Omega + \gamma) + R(B+2C\lambda)\epsilon\frac{d^2U}{d\xi^2}\right]}{1 + \frac{2\epsilon}{\Omega}(B+2C\lambda)R\frac{dU}{d\xi}} \tag{31}$$

where

$$R = \text{Reynolds number} = \frac{u_o l}{\nu} = \text{constant}$$

and

$$U = \frac{u_1}{u_o}; \quad \xi = \frac{r}{l}; \quad \epsilon = \left(\frac{\delta}{l}\right)^2$$

Equation (31) is seen to be an ordinary, first-order, nonlinear differential equation and can be solved numerically for any known pressure distribution, as long as laminar separation does not occur. Since all the quantities on the right side of the equation are known at the beginning of the ramp, the initial rate of growth (the derivative) can be calculated directly from the equation. Then, applying this rate of growth over a small increment of length, a new value of boundary-layer thickness is obtained which can be used again in equation (31) to calculate a new rate of growth. By repeating this procedure, the boundary-layer thickness can be determined over the entire ramp length. The solution of equations of this type is discussed in appendix A.

Turbulent Case

If the velocity u is properly redefined, equations (27) and (28) can be applied to the case of the completely turbulent boundary layer. Thus, if u is interpreted as the mean velocity at a height y in the boundary layer, and if the shape parameter $H = \delta^*/\theta$ is introduced,[7] equation (28) becomes

$$\frac{d\theta}{dr} + \left[\frac{1}{u_1}\frac{du_1}{dr}(H + 2) + \frac{1}{r}\right]\theta = \frac{\tau_o}{\rho u_1^2} \tag{32}$$

This equation reduces to the familiar two-dimensional momentum equation for the case when r is infinite, and to the equation derived in reference 5 for conditions along the center line. The general equation has also been derived in reference 6.

Until a rational theory is developed which gives the velocity distribution through the turbulent boundary layer and the corresponding skin friction, empirical relationships must be used to link H and τ with θ. By use of the method of reference 7, equation (32) can be put into dimensionless form by the following transformations:

$$\chi = R^{1/4}\left(\frac{\theta}{l}\right)^{5/4}$$

$$\zeta = \frac{\tau}{\rho u_1^2}\left(\frac{u_1\theta}{\nu}\right)^{1/4}$$

If these substitutions are made in equation (32), in addition to the dimensionless quantities already introduced for the previous case, the final expression becomes

$$\frac{d\chi}{d\xi} + \frac{5}{4}\left[\frac{1}{U}\frac{dU}{d\xi}(H + 2) + \frac{1}{\xi}\right]\chi = \frac{5}{4}\frac{\zeta}{U^{1/4}} \tag{33}$$

Equation (33) can now be solved for any given pressure distribution by using the variations of H and ζ with ξ which are furnished by

[7] The applicability of such a parameter to radial flows has been justified experimentally by Kehl (reference 5).

reference 7 in which it is established that both are functions of Λ only, where (in this case)

$$\Lambda = \left(\frac{u_1\theta}{\nu}\right)^{1/4} \left(\frac{du_1}{dr}\frac{\theta}{u_1}\right)$$

These curves are reproduced in figure 4.[8] Thus, equation (33) furnishes a differential equation for the growth of the fully turbulent boundary layer along the divergent-ramp floor. This equation, being of the same form as equation (31), can also be solved numerically. (See appendix A.)

Other methods have been proposed for solving equation (32) which range from assuming that H is constant with ξ to using a rather involved expression for the variation of H with ξ. The latter method (see reference 8) is useful for cases in which separation is approached.

Laminar-Turbulent Case

A solution for the case involving transition from the laminar to the turbulent boundary layer can be obtained by combining the cases already discussed. That is, the boundary-layer growth can be calculated up to the point of transition by equation (31) and after complete transition by equation (33). To complete the solution, some information is required regarding the occurrence of transition. Since there is at present no satisfactory theory for predicting the location and manner of transition, it will be necessary in application to make some appropriate assumptions, such as:

1. Sudden transition from a laminar profile of the Pohlhausen type to a fully turbulent boundary layer at some reasonable location such as the minimum-pressure station on the ramp

2. No discontinuity in momentum thickness at the point of transition

Under these conditions, the boundary layer momentum thickness can be calculated over the entire ramp floor (if separation does not occur) by using the momentum thickness (as found by equations (31) and (29)) at the assumed transition point to determine the initial value for the integration of equation (33).

[8]Note that it has been assumed that the relationship given in reference 7 can be applied to the case of radial flow.

It can be seen in the foregoing analysis that equations (31) and (33) can be applied to the case of the convergent ramp if a radial flow is assumed and the distance r is now measured in the upstream direction from the point of convergence. Furthermore, if it is noted that along the center line of the converging or diverging flow $1/r = 1/x = (1/b)(db/dx)$, it can be concluded that divergence has an effect on the boundary layer which is analogous to that of a favorable pressure gradient. Thus, the boundary-layer growth is retarded by divergence while it is accelerated by convergence. This phenomenon has been illustrated by wind-tunnel measurements of the boundary-layer growth along the center lines of parallel-walled and divergent-walled ramps. A comparison of such measurements is presented in figure 5 which has been reproduced from reference 1.

Boundary-Layer Pressure Losses

From the equations just developed, one can calculate the boundary-layer thickness at any station on the ramp floor. The quantity of primary interest in determining the efficiency of an air inlet, however, is the dynamic-pressure-recovery ratio $1 - \overline{\Delta H}/q_o$. Therefore, a relationship will be established between the boundary-layer thickness at the duct entrance and the loss in total pressure due to the boundary layer. Since for a radial flow the boundary-layer thickness is essentially constant across the inlet, this will amount to a two-dimensional analysis.

The total-pressure loss at any point in the boundary layer is

$$\Delta H = \frac{1}{2} \rho \, (u_1^2 - u^2) \tag{34}$$

If the expression for the floor boundary-layer pressure loss is written as

$$\left(\frac{\overline{\Delta H}}{q_o}\right)_{BLF} = \frac{1}{A_D} \int \left(\frac{\Delta H}{q_o}\right) dA = \frac{1}{\frac{1}{2} \rho u_o^2 d} \int_o^\delta \Delta H \, dy \tag{35}$$

where d is the depth of the duct entrance (see fig. 5), the integral can be evaluated by noting, from the expressions previously given for θ and δ^*, that

$$\int_o^\delta \rho u \, dy = \rho u_1 (\delta - \delta^*)$$

and

$$\int_0^{\delta} \rho u^2 \, dy = \rho u_1^2(\delta - \delta^* - \theta)$$

With these relationships, equation (35) reduces to

$$\left(\frac{\overline{\Delta H}}{q_0}\right)_{BLF} = \frac{1}{d}\left(\frac{u_1}{u_0}\right)^2 (\theta+\delta^*) = \frac{\theta}{d}\left(\frac{u_1}{u_0}\right)^2 (1+H) \qquad (36)$$

Thus, if the boundary-layer thicknesses θ and δ^* are determined from equations (29), (31), and (33), the loss in dynamic-pressure recovery due to boundary layer on the ramp floor can now be calculated for any of the three possible conditions considered - the completely laminar case, the fully turbulent case, or the case involving transition. Note that the ratio u_1/u_0 of equation (36) is not the same as the mass-flow ratio but is determined by the local pressure coefficient on the ramp floor.

If it is desired to calculate the boundary-layer pressure loss at one station (say the duct entrance) without determining the boundary-layer growth over the entire ramp length, the calculations can be greatly simplified by using the approximations first introduced by Falkner (reference 9) regarding the shape parameter H and the shear stress τ_0. By this expedient, one can integrate the momentum equation directly to obtain an expression for the boundary-layer momentum thickness at the desired station in terms of the initial momentum thickness and the velocity distribution over the ramp.

Since Falkner's integration was performed on the two-dimensional momentum equation, the method will be extended here to the case of radial flow. The momentum equation in the form of equation (32)

$$\frac{d\theta}{dr} + \left[\frac{1}{u_1}\frac{du_1}{dr}(H+2) + \frac{1}{r}\right]\theta = \frac{\tau_0}{\rho u_1^2} \qquad (32)$$

can be simplified by introducing the shear stress relationship suggested by Falkner

$$\frac{\tau_o}{\rho u_1^2} = \frac{k}{R_\theta^n} = \frac{k\nu^n}{\theta^n u_1^n}$$

Equation (32) can now be written (in dimensionless form) as

$$\frac{d\Theta}{d\xi} + \left[\frac{1}{U}\frac{dU}{d\xi}(H + 2) + \frac{1}{\xi} \right]\Theta = \frac{k}{U^n R^n}\Theta^{-n} \tag{37}$$

where

$$\Theta = \frac{\theta}{l}, \quad \xi = \frac{r}{l}, \quad U = \frac{u_1}{u_o}, \quad \text{and} \quad R = \frac{u_o l}{\nu}$$

This differential equation is of the Bernoulli type and can be integrated directly if H is assumed constant. The resulting solution is

$$\Theta_2 = \frac{1}{\xi_2 U_2^{H+2}} \left[(n+1)\frac{k}{R^n}\int_1^2 \xi^{n+1} U^{(H+1)(n+1)+1}\, d\xi + \left(\Theta_1 \xi_1 U_1^{H+2}\right)^{n+1} \right]^{\frac{1}{n+1}} \tag{38}$$

where 1 and 2 refer to the initial and final stations on the ramp. Equation (38) then gives the value of θ (or Θl) to be used in equation (36), if the values of H, k, and n are specified. For the laminar boundary layer $H = 2.592$ (Blasius profile), $k = 0.2205$, and $n = 1$. For the turbulent boundary layer, H is generally assumed to be about 1.5, n about 1/6, and k about 0.0065, although several other values have been suggested. These are discussed further in reference 10.

EFFECTS OF MASS-FLOW RATIO

Much of the analysis thus far presented has been formulated without attention to the presence of the duct entrance. As interest is focused on stations approaching the entrance, consideration must be given to effects brought about by changes in mass-flow ratio. An understanding of the most immediate consequences of changes in mass-flow ratio may be gained by simple continuity considerations.

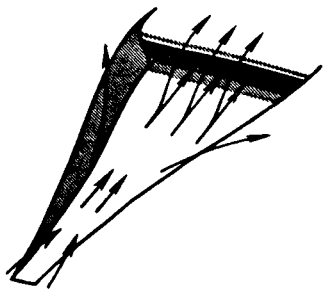

As the mass-flow ratio decreases, more air which would have gone into the duct must spill out over the lip and ramp walls ahead of the entrance, as shown in the sketch. Since the vortex filaments must follow the paths of the streamlines, it is apparent that the vortices may not be completely swallowed by the duct. In fact, as the vortices approach the duct entrance, they must, at very low inlet velocities, pass over the lip and outside the duct.

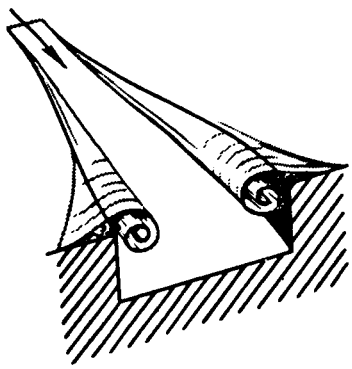

In order for the vortices to move away from the ramp floor at stations near the duct lip, the vortex sheets must leave the ramp walls at increasing angles until finally they break away from the main surface as shown in the sketch. When the vortex sheet leaves the surface in this manner, a region of secondary vortical flow introducing additional pressure losses appears over the main surface just outside the inlet. In the extreme case, a distinct secondary pair of vortices may be formed in these regions rotating in a sense opposite to that of the primary pair. These additional losses are a function of the mass-flow ratio and the ramp divergence and may be expected to decrease with increasing divergence and with increasing mass-flow ratio. Since these losses occur on the main surface, however, in regions where the flow is directed away from the inlet, they cannot enter the duct and must appear as external drag. Thus, there are, in general, three important direct consequences of reducing the mass-flow ratio: (1) Due to the increased adverse pressure gradient, the floor boundary layer is thickened and may separate; (2) the rolled-up vortices are moved farther away from the ramp floor and may move entirely outside the duct; and (3) regions of separated or vortical flow may appear on the main surface near the ramp edges. This third effect is augmented by the fact that the vortices cause the outboard sections of the lip to operate at a higher angle of attack than the center section. This tends to produce regions of separated flow above the outer edges of the lip, particularly at low mass-flow ratios where the angle of attack of the entire lip is increased.

Since any pressure losses that are not taken internally must appear as external drag, several interesting observations can be made regarding the variations of ram recovery and external drag with mass-flow ratio. Of the three effects of mass-flow ratio enumerated above, the first and third both represent increased losses as the mass-flow ratio is reduced.

However, the floor boundary-layer loss is entirely internal while the main surface separation losses are entirely external. The vortices, on the other hand, represent a loss which is relatively constant with mass-flow ratio but is sometimes taken internally and sometimes taken externally. With this information the variations of ram recovery (or loss) at the duct entrance and external drag with mass-flow ratio can be predicted qualitatively, as shown in the following sketch for a given divergent-ramp inlet:

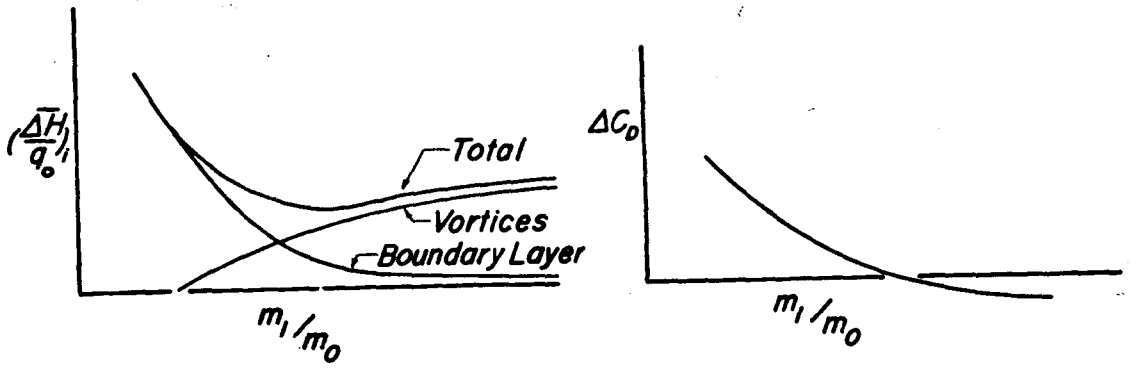

Since part of the losses swallowed by the duct at high mass-flow ratios arise from boundary layer taken from the fuselage surface, the incremental external drag may be expected to become negative as shown. In fact, an expression can now be written for the total-pressure loss contributing to external drag:

$$\left(\frac{\overline{\Delta H}}{q_o}\right)_e = (1 - C)\left[\left(\frac{\overline{\Delta H}}{q_o}\right)_V + \left(\frac{\overline{\Delta H}}{q_o}\right)_{BLS}\right] + \left(\frac{\overline{\Delta H}}{q_o}\right)_{SEP} - \left(\frac{\overline{\Delta H}}{q_o}\right)_{BLC} \quad (39)$$

where $(\overline{\Delta H}/q_o)_{BLC}$ refers to the boundary-layer-control action which the inlet performs on the fuselage, while $(\overline{\Delta H}/q_o)_{SEP}$ represents the loss due to separation of the fuselage boundary layer near the ramp edges.

The curve shown in the preceding sketch for the variation of floor boundary-layer loss can be calculated by the use of equations (36) and (38) if the ramp pressure distribution is known for each mass-flow ratio. The maximum value for the vortex loss curve is given by $1/2\pi A_D\,(\Gamma/u_o)^2$ (equation (23)), while the values at lower mass-flow ratios depend upon the portion C of the vortices which is swallowed by the duct. This quantity depends upon the actual size and location of the vortex cores, which have not been determined theoretically. Therefore, an experiment was conducted which will aid is establishing

the desired information. (The tests will be discussed and the results presented in a later section.) It can be seen from the loss curves of the foregoing sketch that there will be an optimum mass-flow ratio at which the combined loss in ram recovery due to vortices and boundary layer is a minimum.

It will be noted that the losses due to vortices and floor boundary layer have been added directly to obtain the total loss in ram recovery. This raises the question of interaction between the vortices and the floor boundary layer. It was pointed out in the earlier discussion that the vortices cause the boundary layer to thin near the center of the ramp and thicken near the walls. In addition, there will be some tendency for a portion of the thickened floor boundary layer near the ramp walls to become entrained in the vortices. The magnitude of these effects on the total losses will probably be small.

Another boundary-layer phenomenon that has not yet been discussed is the entrainment of fuselage boundary layer into the vortex cores. The total-pressure loss due to this entrainment $\left(\overline{\Delta H}/q_o\right)_{BLS}$ can be expressed in equation form if the width of fuselage surface from which boundary layer enters one vortex is denoted by s:

$$\left(\frac{\overline{\Delta H}}{q_o}\right)_{BLS} = \frac{1}{A_D}\left[2s\int_o^{\delta}\left(\frac{\Delta H}{q_o}\right)dy\right] \tag{40}$$

The integral in equation (40) has been evaluated previously (equations (35) and (36)), so that equation (40) reduces to

$$\left(\frac{\overline{\Delta H}}{q_o}\right)_{BLS} = \frac{2\theta s}{A_D}(1+H)\left(\frac{u_1}{u_o}\right)^2 \tag{41}$$

Note that in this instance θ and u_1 are measured just ahead of the inlet ramp. Equation (41) requires, of course, that the boundary layer does not separate at the ramp edges (as discussed previously).

The distance s will actually depend on the mass-flow ratio, increasing with increasing mass-flow ratio. An estimate of the order of magnitude of the loss $\left(\overline{\Delta H}/q_o\right)_{BLS}$ can be obtained by taking s to be the projection of the ramp wall in the stream direction; that is,

$$2s = b_{x=l} - b_{x=0}$$

in which case equation (41) would become

$$\left(\frac{\overline{\Delta H}}{q_o}\right)_{HLS} \approx \frac{\theta}{A_D}(1+H)\left(\frac{u_1}{u_o}\right)^2\left(b_{x=l}-b_{x=0}\right) \qquad (42)$$

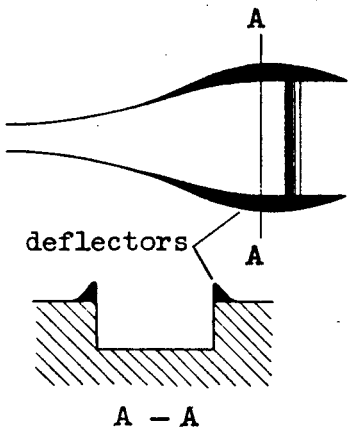

The losses due to the vortices and entrained boundary layer give rise to the question of possible methods for reducing these losses in the duct entrance. Since the portion of these losses entering the duct is determined by the relative positions of the duct lip and the vortices, the obvious method of accomplishing the desired result is either to submerge the lip deeper into the fuselage, or to force the vortices farther away from the ramp floor by the use of "deflectors." (See sketch.) It should be realized, however, that either of these expedients can at best only convert internal pressure losses to external drag. Furthermore, each method has additional disadvantages which might cancel entirely the beneficial effect on recovery. If the lip is further submerged, the boundary-layer thickness on the floor will then represent a larger portion of the duct depth, thus increasing $(\overline{\Delta H}/q_o)_{BLF}$. If, on the other hand, the vortices are moved out, then their beneficial effect in discouraging thickening and separation of the floor boundary layer is reduced. Thus, the designer must exercise great care in the choice of methods for increasing the pressure recovery of a submerged inlet.

EFFECTS OF COMPRESSIBILITY

The entire analysis presented in this paper has been for an incompressible fluid (M=0). However, some pertinent observations can be made regarding the effects of compressibility on the pressure losses considered.

Studies of slender wings and bodies at small angles of attack have shown that the effect of Mach number becomes negligibly small as the slenderness is increased. Similarly, for the slender ramp plan forms customarily used in submerged inlets, the vortex losses, which result primarily from flows in the transverse planes, can be expected to show little effect of Mach number.

The boundary-layer growth is associated primarily with the longitudinal flow which is influenced by compressibility to a greater degree than are the transverse flows. In particular, pressure gradients become steeper with increasing Mach number. In the case of the submerged inlet, where the pressure gradient is adverse over most of the ramp length, an increase in boundary-layer thickness may be expected with increasing Mach number due to the change in pressure distribution. On the other hand, for a fixed pressure distribution, a decrease in boundary-layer thickness is indicated due to local viscosity changes brought about by aerodynamic heating. Since this latter effect is known to be small at subsonic speeds, the effect of compressibility can be almost entirely taken into account by using (as demonstrated in reference 11) the actual compressible pressure distribution in the incompressible boundary-layer equations. It is therefore concluded that the analysis presented in this report can be applied with reasonable accuracy to compressible flows at subcritical Mach numbers.

In considering effects on the ram pressures due to increasing Mach number, care must be taken in the definition of ram recovery, since the reference quantity $\frac{1}{2}\rho u_o^2$ upon which the inlet efficiency is based at low speeds no longer represents the actual available ram pressure at the higher Mach numbers. In fact, if the inlet efficiency is based upon $\frac{1}{2}\rho u_o^2$ at higher Mach numbers, efficiencies in excess of 100 percent may be obtained, purely as a result of the failure to account for the increase in available ram pressure. Such a difficulty is generally overcome by discarding the approximation of equation (1) and dealing with the quantity $(H_1 - p_o)/(H_o - p_o)_{av}$ which is called the ram recovery ratio. This quantity differs from the dynamic-pressure recovery ratio $1 - \frac{\overline{\Delta H}}{q_o}$ by the compressibility factor $F=1+\eta^* = 1+ \frac{M^2}{4} + \frac{M^4}{40} + \ldots$, so that at low speeds the two efficiencies are identical, as indicated in equation (1). These and other related quantities are discussed in reference 12.

WIND-TUNNEL EXPERIMENT

A brief wind-tunnel test was conducted in the Ames 7- by 10-foot wind tunnel to study experimentally the vortex pressure losses discussed in this paper. A large-scale inlet of linear geometry was mounted in a false wall which allowed the tunnel-wall boundary layer to pass beneath it, and measurements were made of the total-pressure losses outside the ramp floor boundary layer, both inside and outside the duct entrance. The model and installation of total-pressure rakes are illustrated in figure 6. Distributions of total-pressure recovery were obtained over the mass-flow ratio range for a number of ramp divergences, keeping the duct entrance area and ramp length constant. A typical distribution is shown schematically in figure 7. It should be noted that the maximum angularity of the flow in the vortices was of the order of 15°; consequently, the error in total-pressure measurements is believed to be small.

By this means, it was possible to obtain the approximate locations of the centers of the vortices, and to measure the integrated total-pressure loss due to the vortices and the main surface boundary layer entrained in the vortices, and the portion of that loss which entered the duct. The results are given in figures 8 and 9. At the lower mass-flow ratios, flow separation occurred on the main surface and it is believed that the failure to distinguish this loss from the losses in the vortices is responsible for the apparent variation of total vortex loss with mass-flow ratio. An important point regarding figure 8 is that $(\overline{\Delta H}/q_o)_V + (\overline{\Delta H}/q_o)_{BLS}$ does not go to zero at zero divergence. This is in keeping with the analysis since there should be a vortex loss proportional to the ramp angle α which was held constant in the test.

It should be pointed out that the variation of the fraction C with mass-flow ratio (fig. 9) depends somewhat upon the shape of the duct lip, as well as upon its vertical location. Such influences were not investigated.

Since the pressure losses measured in the vortex regions include $(\overline{\Delta H}/q_o)_{BLS}$, it is not advisable to use these data with equation (23) to determine the unknown function $g(\omega/\alpha)$ of equations (10) and (11). The actual determination of this function would require detailed measurements of the magnitude of the circulation over the entire range of mass-flow ratios and ramp divergences.

CONCLUDING REMARKS

A theoretical study has been made of the flow in submerged air inlets in order to determine the effects of some of the important design parameters on the ram-recovery characteristics of the inlets at low speeds. Inlets having parallel, divergent, and convergent ramp walls have been considered and their fundamental differences discussed. As a result of the analysis presented, the integrated total-pressure loss in the entrance of a three-dimensional submerged air inlet has been broken down into its essential components which can now be calculated subject to the restrictions discussed in the foregoing sections.

In general, the major total-pressure loss taken internally at the duct entrance can be expressed as

$$\left(\frac{\overline{\Delta H}}{q_o}\right)_i = \left(\frac{\overline{\Delta H}}{q_o}\right)_{BLF} + C\left[\left(\frac{\overline{\Delta H}}{q_o}\right)_V + \left(\frac{\overline{\Delta H}}{q_o}\right)_{BLS}\right]$$

where C is primarily a function of the mass-flow ratio. Some experimental values of this function have been given in figure 9 for several

ramp divergences. Equations have been developed in this report for calculating the other quantities contributing to $\left(\overline{\Delta H}/q_o\right)_i$.

Similarly, the major total-pressure loss taken as external drag can be expressed as

$$\left(\frac{\overline{\Delta H}}{q_o}\right)_e = (1 - C)\left[\left(\frac{\overline{\Delta H}}{q_o}\right)_V + \left(\frac{\overline{\Delta H}}{q_o}\right)_{BLS}\right] + \left(\frac{\overline{\Delta H}}{q_o}\right)_{SEP} - \left(\frac{\overline{\Delta H}}{q_o}\right)_{BLC}$$

where $\left(\overline{\Delta H}/q_o\right)_{BLC}$ represents the reduction in external drag due to the boundary-layer-control action of the inlet on the fuselage, while $\left(\overline{\Delta H}/q_o\right)_{SEP}$ represents the loss due to separation of the fuselage boundary layer at the ramp edges. Neither of these two quantities has been determined, although their dependence on the mass-flow ratio has been discussed.

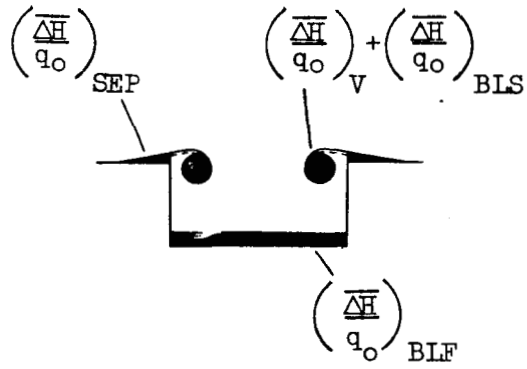

The regions of total-pressure loss that have been considered in this report are shown schematically in cross section in the sketch.

It was found that divergence of the ramp walls has two major effects on the ram-recovery characteristics of the submerged inlet. On the one hand, a vortex pair is created in the inlet which introduces an additional source of pressure loss - the vortex cores. On the other hand, the ramp wall divergence creates a favorable effect on the boundary-layer growth along the ramp floor, thus reducing the pressure loss due to the boundary layer.

The equations developed in the analysis indicate that the pressure loss in the vortex cores is determined approximately by the inlet geometry, while the portion entering the duct entrance depends primarily upon the mass-flow ratio and the shape and location of the duct lip. Due to the nature of the flow field created by the rolled-up vortex sheets in the inlet, a measurement of ram recovery in the plane of the duct center line can be taken only as an indication of the minimum boundary-layer thickness on the ramp floor. Such a measurement is therefore inadequate for predicting the ram-recovery characteristics of a submerged inlet having a divergent ramp.

A method has been presented for calculating the boundary-layer growth along the ramp floor for parallel, divergent, and convergent ramp walls, for a known ramp pressure distribution. It was found that the

effect on the growth of this boundary layer due to divergence of the ramp walls is analogous to that of a favorable pressure gradient. Convergence has a corresponding adverse effect.

Since the boundary-layer losses on the floor decrease with increasing mass-flow ratio while the internal vortex losses increase with increasing mass-flow ratio, there must be an optimum mass-flow ratio for which the combined losses in ram recovery are a minimum. By the same reasoning, it can be concluded that there must be an optimum divergence angle for a straight ramp which will give minimum total-pressure losses.

The total vortex pressure loss was found to depend upon the inlet geometry and the local pressure coefficient, and to a lesser extent upon the mass-flow ratio. The ramp boundary-layer losses are determined by the momentum thickness, the local pressure coefficient, and the boundary-layer-shape parameter.

Ames Aeronautical Laboratory,
National Advisory Committee for Aeronautics,
Moffett Field, Calif., Jan. 12, 1951.

APPENDIX A

SOLUTION OF THE BOUNDARY-LAYER GROWTH EQUATIONS

Since equations (31) and (33) are both of the general form

$$\frac{dy}{dx} = f(x,y) \tag{A1}$$

they can be solved by one of the standard numerical methods of integration. Such a method consists, generally, of determining from equation (A1) the derivative or slope dy/dx for the given initial values of x and y (in the present case, this amounts to specifying the boundary-layer thickness at the beginning of the ramp) and using that slope over a small increment of x to determine the next value of y, and thereby the next value of dy/dx. This procedure is repeated until the function y has been evaluated over the desired range of x. The following table outlines a systematic method in which the error due to taking finite increments of x is kept relatively small. Naturally, the accuracy of the integration will be impaired if the increments of x chosen are too large.

x	y	f	f×h	
x_0	y_0	$f(x_0, y_0)$	k_1	$\Sigma = \frac{1}{2}(k_1 + k_4)$
$x_0 + \frac{h}{2}$	$y_0 + \frac{k_1}{2}$	$f(x_0 + \frac{h}{2}, y_0 + \frac{k_1}{2})$	k_2	$+ k_2 + k_3$
$x_0 + \frac{h}{2}$	$y_0 + \frac{k_2}{2}$	$f(x_0 + \frac{h}{2}, y_0 + \frac{k_2}{2}$	k_3	$- - -$
$x_0 + h$	$y_0 + k_3$	$f(x_0 + h, y_0 + k_3)$	k_4	$k = \frac{1}{3}\Sigma$
$x_1 = x_0 + h$	$y_1 = y_0 + k$			

h = increment of x chosen for integration

The above table has been reproduced from reference 13.

REFERENCES

1. Dryden, Hugh L.: The Aeronautical Research Scene – Goals, Methods, and Accomplishments. (37th Wilbur Wright Lecture) Jour. Roy. Aero. Soc., vol. 53, no. 463, July 1949, pp. 623–666.

2. Prandtl, L.: Tragflügeltheorie, I Mitteilung. Nachrichten der K. Gesellschaft der Wissenschaften zu Gottingen, Mathematisch–physikalische Klasse, S. 451–477, 1918. Reprinted in Prandtl, L., and Betz, A.: Vier Abhandlungen zur Hydrodynamik und Aerodynamik, Göttingen, 1927. Reprinted by Edward Brothers, Inc., 1943.

3. Goldstein, Sydney, ed.: Modern Developments in Fluid Dynamics, vol. I, The Clarendon Press (Oxford), 1938.

4. Prandtl, L.: The Mechanics of Viscous Fluids. Vol. III, div. G, sec. 17, of Aerodynamic Theory, W. F. Durand, ed., Julius Springer (Berlin), 1935, pp. 102–112.

5. Kehl, A.: Investigations on Convergent and Divergent Turbulent Boundary Layers. British Ministry of Aircraft Production, R.T.P. Translation No. 2035. (Translation of: Ingenieur – Archiv, Bd. 13, Heft 5, 1943, pp. 293–329.)

6. Tetervin, Neal: Boundary–Layer Momentum Equations for Three–Dimensional Flow. NACA TN 1479, 1947.

7. Howarth, L.: The Theoretical Determination of the Lift Coefficient for a Thin Elliptic Cylinder. Proceedings of the Royal Society of London, Series A, vol. 149, 1935, pp. 558–586.

8. von Doenhoff, Albert E., and Tetervin, Neal: Determination of General Relations for the Behavior of Turbulent Boundary Layers. NACA Rep. 772, 1943.

9. Falkner, V. M.: A New Law for Calculating Drag. The Resistance of a Smooth Flat Plate with Turbulent Boundary Layer. Aircraft Engineering, vol. XV, no. 169, March 1943, pp. 65–69.

10. Tetervin, Neal: A Method for the Rapid Estimation of Turbulent Boundary–Layer Thickness for Calculating Profile Drag. NACA ACR L4G14, July 1944.

11. Allen, H. Julian, and Nitzberg, Gerald E.: The Effect of Compressibility on the Growth of the Laminar Boundary Layer on Low–Drag Wings and Bodies. NACA TN 1255, 1947.

12. Hanson, Frederick H., Jr., and Mossman, Emmet A.: Effect of Pressure Recovery on the Performance of a Jet-Propelled Airplane. NACA TN 1695, 1948.

13. Ince, E. L.: Ordinary Differential Equations. Dover Publications, New York, 1944.

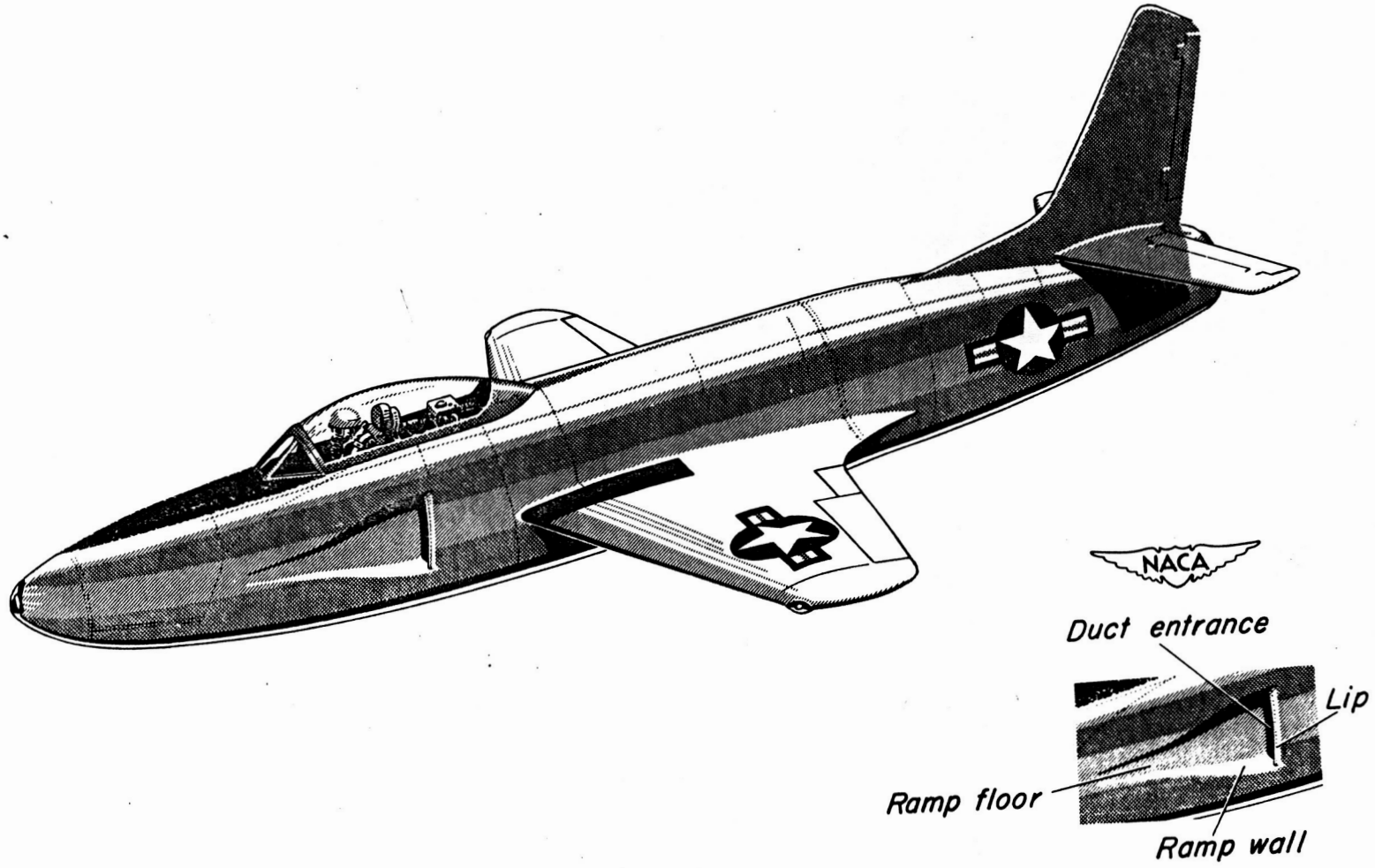

Figure 1.– Typical installation of a submerged inlet in a jet-propelled airplane showing inset of inlet components.

Page intentionally left blank

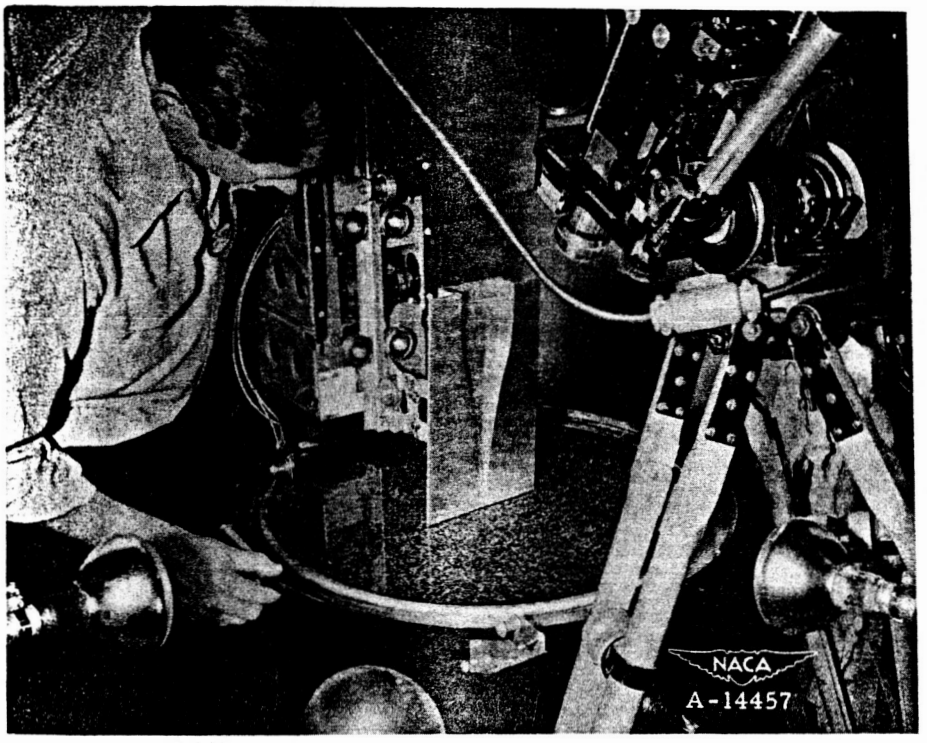

Figure 2.– Closeup of water tank with model mounted in position for starting a run.

Page intentionally left blank

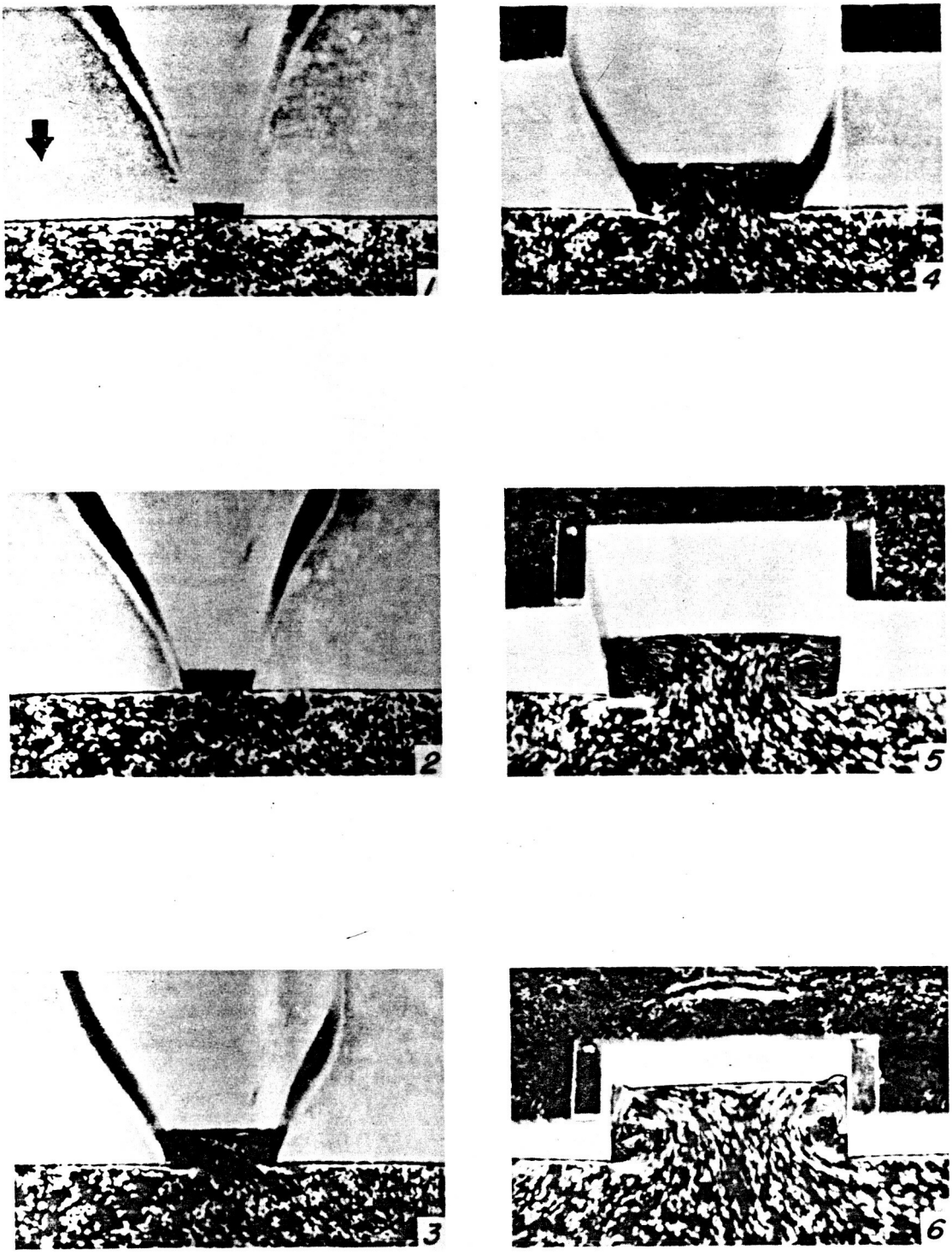

NACA
A-15007

Figure 3.— Photographs of the transverse flow at successive stations in a submerged inlet having divergent ramp walls.

Page intentionally left blank

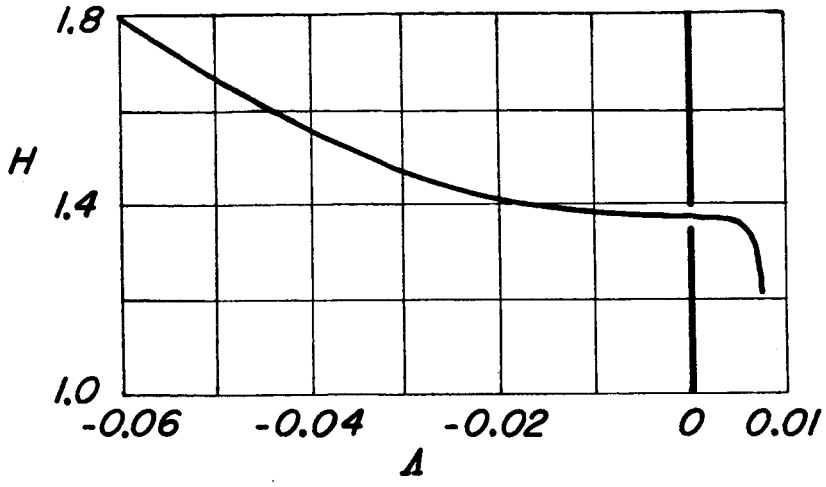

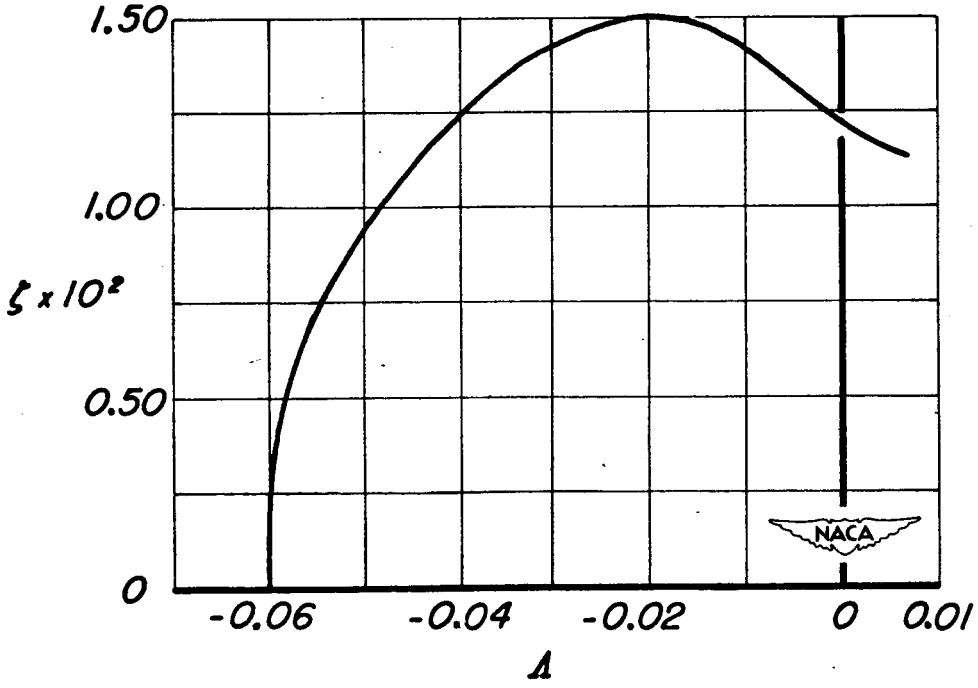

Figure 4.- Variation of boundary-layer-shape parameter and shear-stress variable with parameter Λ involving Reynolds number and pressure gradient (from reference 7).

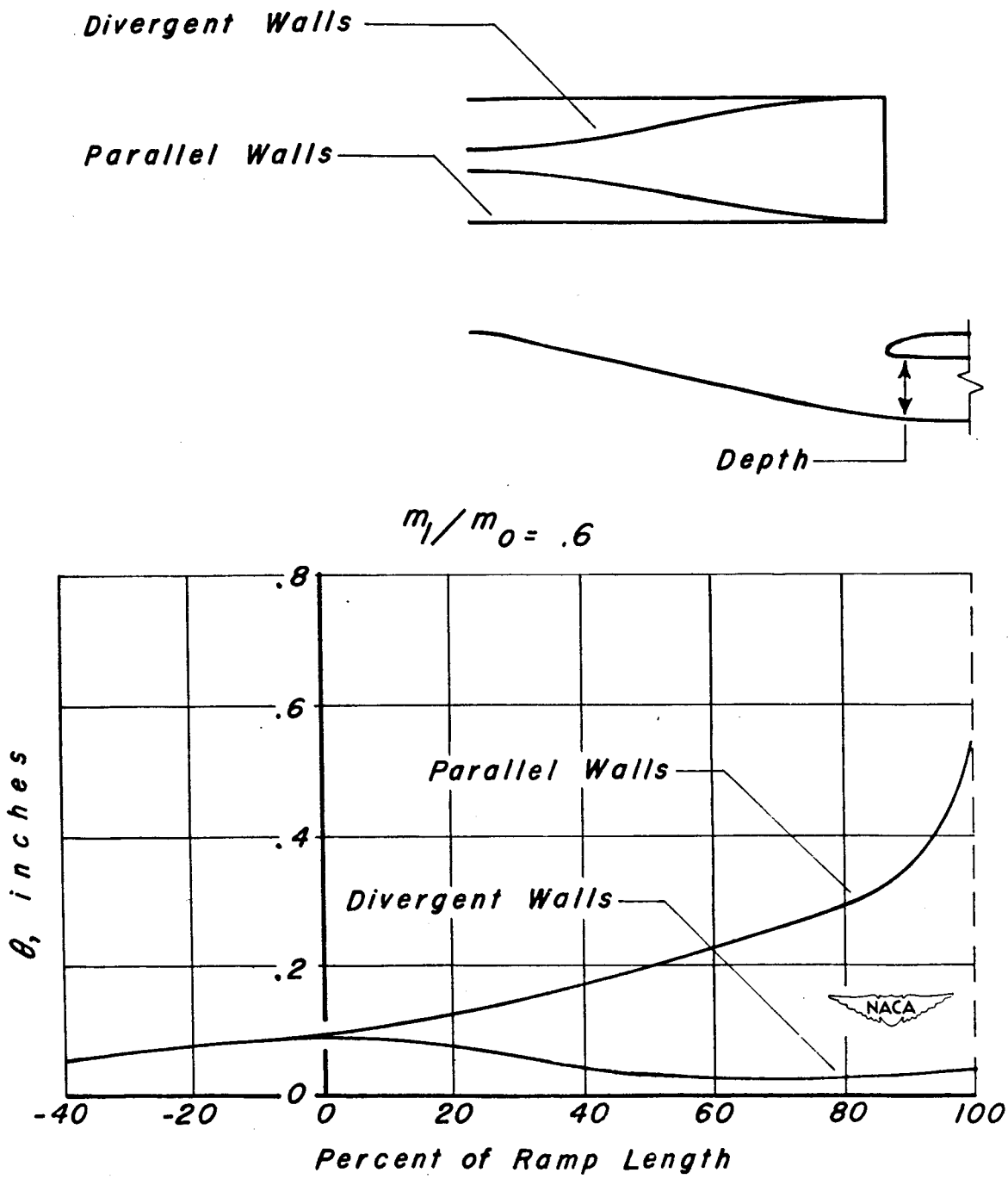

Figure 5.- Wind-tunnel measurements of the boundary-layer momentum thickness θ along the center line of submerged inlets having parallel and divergent ramp walls (from reference 1).

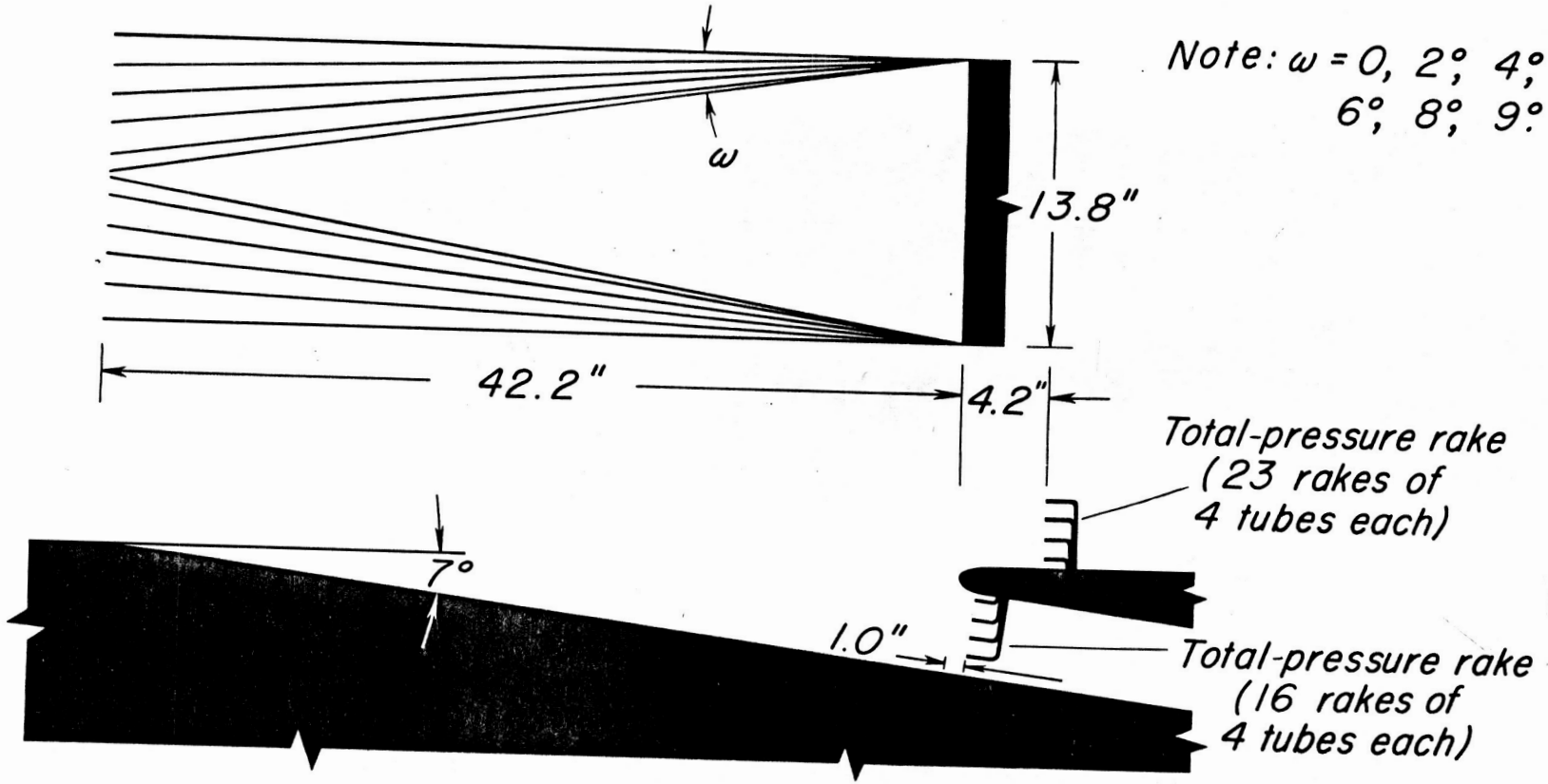

Figure 6.- Schematic sketch of wind-tunnel model showing location of total-pressure rakes.

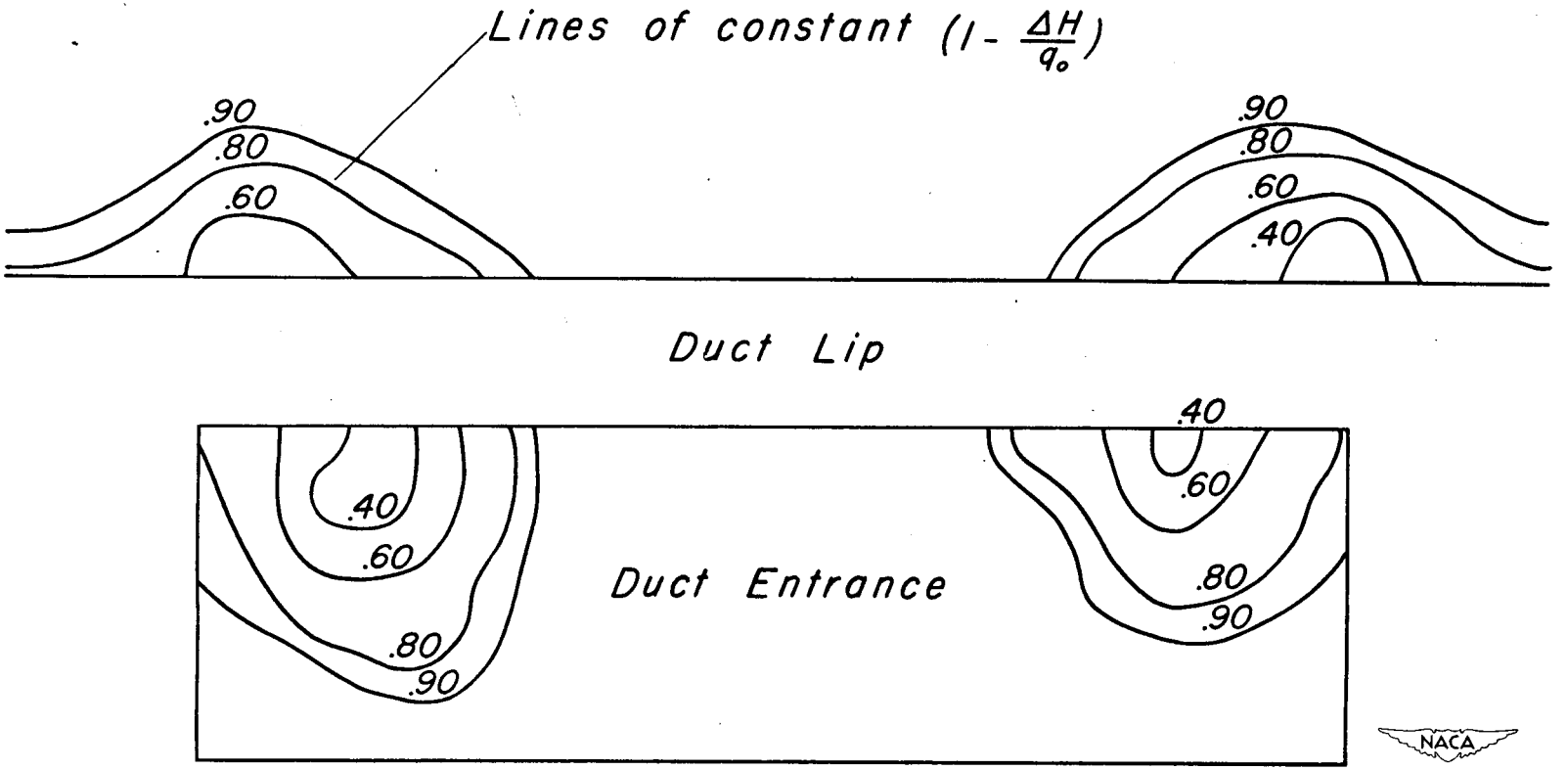

Figure 7.- Typical experimental distribution of total-pressure recoveries in the vortex regions.

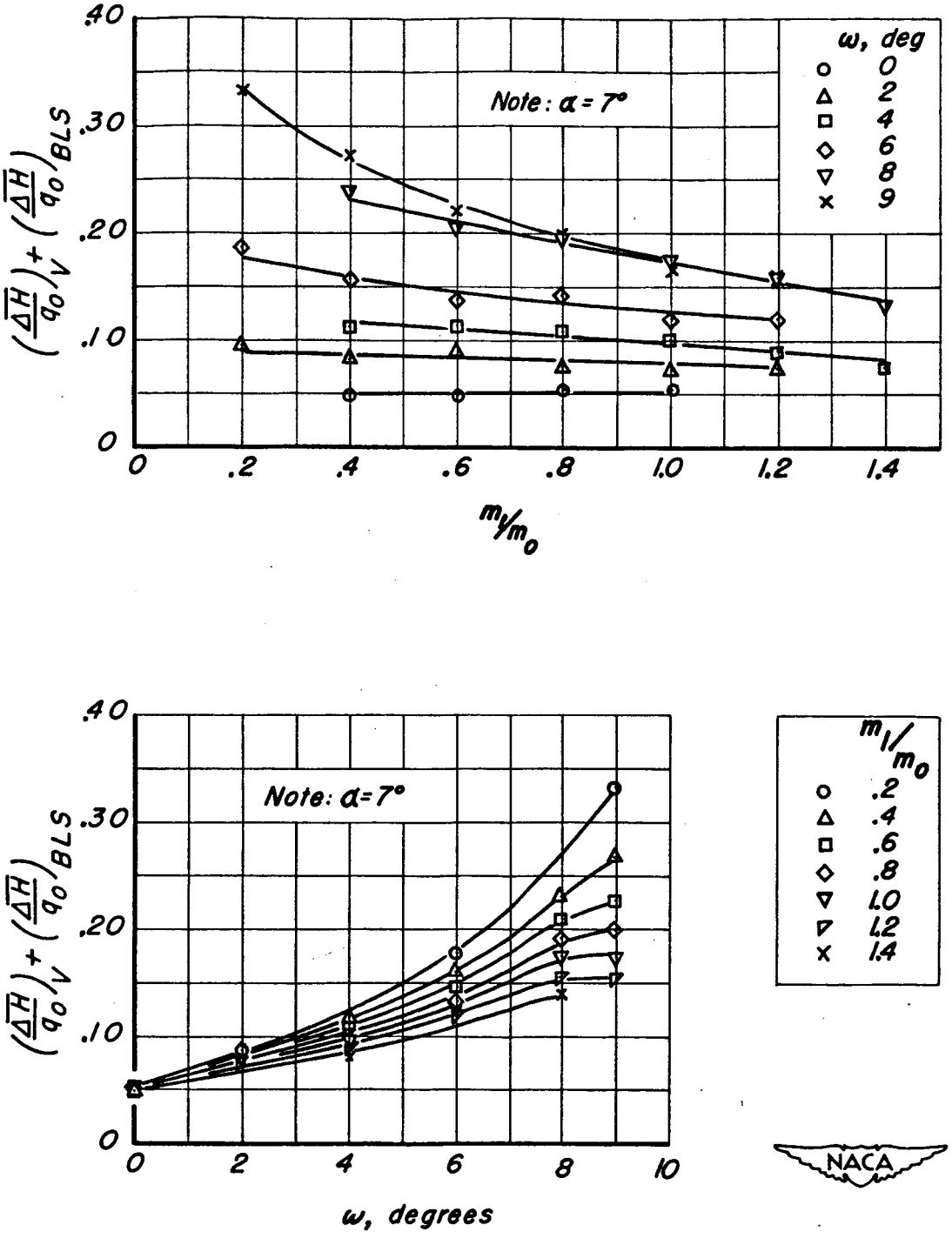

Figure 8.- Wind-tunnel measurements of the variation of total vortex losses with mass-flow ratio and ramp-divergence angle.

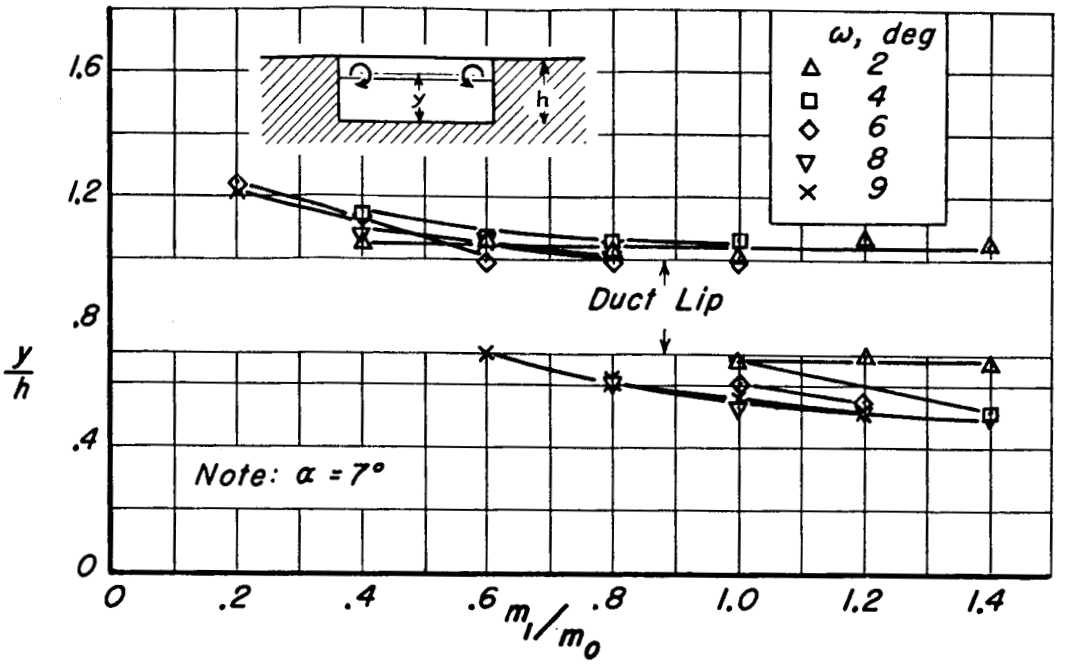

(a) Vertical locations of vortex centers.

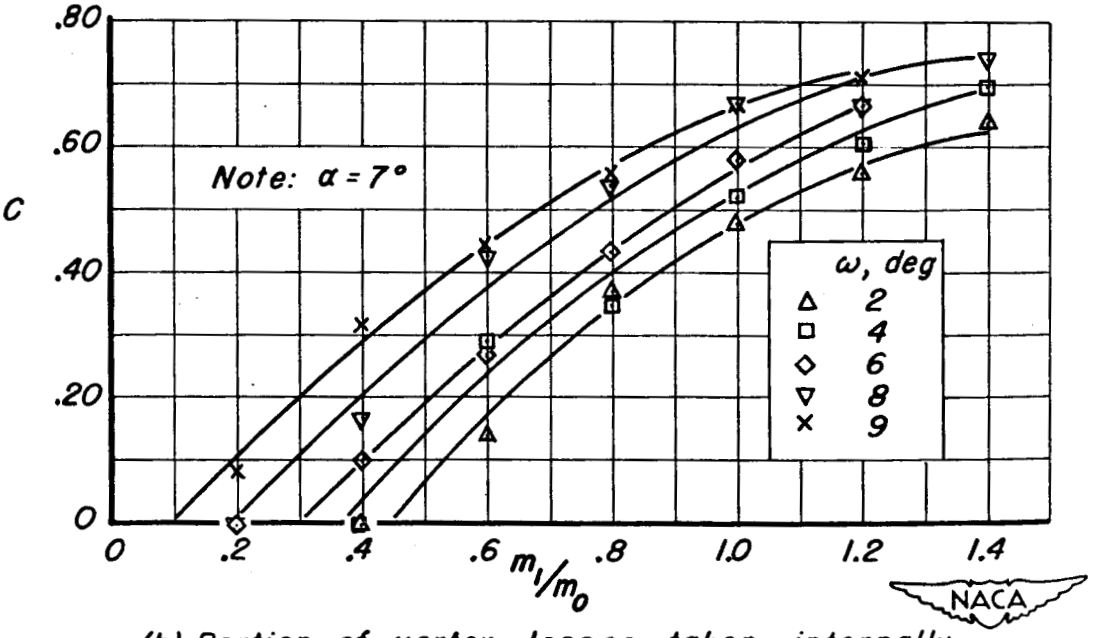

(b) Portion of vortex losses taken internally.

Figure 9.- Wind-tunnel measurements of the variation with mass-flow ratio of the vortex-center locations and the portion of total vortex losses entering the duct.